

Chromosomes Lacking Telomeres are Present in the Progeny of Human Lymphocytes Exposed to Heavy Ions

M. Durante,^a K. George^b and F. A. Cucinotta^{c,1}

^a Department of Physics, University Federico II, 80126 Naples, Italy; ^b Wyle Laboratories, Houston, Texas 77058; and ^c NASA Lyndon B. Johnson Space Center, Houston, Texas 77058

Durante, M., George, K. and Cucinotta, F. A. Chromosomes Lacking Telomeres are Present in the Progeny of Human Lymphocytes Exposed to Heavy Ions. *Radiat. Res.* **165**, 51–58 (2006).

High-charge and energy (HZE) nuclei represent one of the main health risks for human space exploration, yet little is known about the mechanisms responsible for the high biological effectiveness of these particles. We have used *in situ* hybridization probes for cross-species multicolor banding (RxFISH) in combination with telomere detection to compare yields of different types of chromosomal aberrations in the progeny of human peripheral blood lymphocytes exposed to either high-energy iron ions or γ rays. Terminal deletions showed the greatest relative variation, with many more of these types of aberrations induced after exposure to accelerated iron ions (energy 1 GeV/nucleon) compared with the same dose of γ rays. We found that truncated chromosomes without telomeres could be transmitted for at least three cell cycles after exposure and represented about 10% of all aberrations observed in the progeny of cells exposed to iron ions. On the other hand, the fraction of cells carrying stable, transmissible chromosomal aberrations was similar in the progeny of cells exposed to the same dose of densely or sparsely ionizing radiation. The results demonstrate that unrejoined chromosome breaks are an important component of aberration spectra produced by the exposure to HZE nuclei. This finding may well be related to the ability of such energetic particles to produce untoward late effects in irradiated organisms. © 2006 by Radiation Research Society

INTRODUCTION

Most DNA breaks induced in human cells by ionizing radiation are processed within a few hours of exposure and are either rejoined, leaving normal chromosomes, or misrejoined, leading to structural chromosomal aberrations (e.g. 1, 2). Whether a fraction of the initial breaks remain unrejoined indefinitely remains to be determined. It has been shown that after extended incubation, the yield of radiation-induced residual breaks in prematurely condensed

chromosomes usually reaches a plateau that is higher than the control (1), but these types of breaks may include interstitial deletions (intra-arm asymmetrical intrachanges) as well as true terminal deletions with “open” DNA breaks. Most studies using peptide nucleic acid (PNA) telomeric probes show that terminal deletions or incomplete exchanges (leading to a truncated chromosome) are very rare at the first mitosis after exposure to either γ (3) or X rays (4). In contrast, high-charge and energy (HZE) particles are very effective in inducing chromosomal aberrations in human cells (5), and the fraction of both residual prematurely condensed chromosome breaks (6) and true incomplete exchanges (7) is much higher than after sparsely ionizing radiation. However, it remains undetermined whether truncated chromosomes without a telomere can be transmitted through the cell cycle to the progeny of irradiated cells. This is significant because telomere dysfunction has been identified as a primary mechanism involved in the chromosomal instability observed in cancer cells (8). Loss of telomeres can elicit sister chromatid union and the prolonged breakage/fusion/bridge (B/F/B) cycles (9) that have been observed in mouse (10) and human (11) tumors.

All comparisons of chromosomal damage induced by sparsely and densely ionizing radiation are complicated to some extent by the technique employed for the analysis. It is necessary to use different cytogenetic methods to visualize different aberration types, and sparsely and densely ionizing radiation can produce substantially different patterns of aberrations. For instance, a greater fraction of complex rearrangements (12) and intrachromosomal exchanges (13) are induced by α particles than by γ rays. We elected to use rainbow cross-species fluorescence *in situ* hybridization (RxFISH) with flow-sorted, differentially labeled gibbon chromosomes (14) to assess chromosome damage in human lymphocytes exposed to accelerated heavy ions because this method can be used to identify inter- as well as intrachromosomal exchanges in addition to terminal deletions. Owing to the extensive homology between human and gibbon DNA and to the many chromosomal rearrangements that have occurred during evolution, RxFISH results in a specific color banding for each human chromosome. The gibbon DNA probes are labeled with three different

¹ Address for correspondence: NASA Johnson Space Center, Houston TX, 77058; e-mail: Francis.A.Cucinotta@nasa.gov.

fluorochromes (Cy3, Cy5 and FITC), generating seven different colors and approximately 90 bands in the human haploid genome. We applied RxFISH to human peripheral blood lymphocytes exposed *in vitro* at the NASA Space Radiation Laboratory at Brookhaven National Laboratory to either ^{137}Cs γ rays or 1 GeV/nucleon iron ions with a linear energy transfer (LET) of about 147 keV/ μm .

MATERIALS AND METHODS

Blood Samples

Venous blood from a healthy male volunteer was drawn into a sodium-heparinized Vacutainer. The volunteer gave informed consent for his blood sample to be used in these experiments, and the protocol was approved by the Institutional Review Board (IRB) at Brookhaven National Laboratory (Upton, NY). The blood was transferred into 15-ml Falcon conical centrifuge tubes and irradiated within 2 h of the blood drawing.

Irradiations

Whole blood was exposed at room temperature to γ rays using a ^{137}Cs source or to accelerated $^{56}\text{Fe}^{26+}$ ions using the NASA Space Radiation Laboratory facility at Brookhaven National Laboratory. The dose rate was approximately 1 Gy/min in both experiments, and the dose was 0.3, 1 or 3 Gy ($\pm 5\%$). The physical characteristics and dosimetry of the 1 GeV/nucleon ^{56}Fe -ion beam have been described in detail by Zeitlin *et al.* (15). The dose-averaged LET of this beam is approximately 147 keV/ μm , which is around the peak of effectiveness for charged particles (5). Samples were processed within 1 h of exposure, as described below.

In Vitro Growth

Blood was diluted 1:20 in RPMI 1640 medium (Gibco-BRL, Grand Island, NY), supplemented with 20% calf serum, 2% phytohemagglutinin, 1% L-glutamine, 1% penicillin/streptomycin, 0.1% sodium heparin (stock 176.2 U/mg), 5 $\mu\text{g}/\text{ml}$ bromodeoxyuridine (BrdU) (Sigma), and 5 $\mu\text{g}/\text{ml}$ deoxycytidine (Sigma) and incubated in 25-cm² tissue culture flasks at 37°C in the vertical position in a humidified atmosphere of 95% air/5% CO₂. The cultures were shaken gently every day. After 142 h incubation, Colcemid (Gibco-BRL) was added to the cultures at a final concentration of 0.1 $\mu\text{g}/\text{ml}$, and the cells were incubated for a further 2 h at 37°C.

Chromosome Preparation

Metaphase spreads were prepared on glass microscope slides using standard cytogenetic methods. Slides were air-dried and then treated for 5 min at 37°C in 0.005% pepsin. Slides were then washed in PBS, fixed for 2 min in 1% formaldehyde, washed again in PBS, and dehydrated in 70%, 85% and 100% ethanol for 2 min each. After air-drying, slides were aged in the dark for 2–3 days at room temperature before denaturation.

RxFISH Hybridization

Cells were hybridized with Harlequin*FISH™ probes (Cambio Ltd, Cambridge, UK) containing gibbon DNA following the basic protocol recommended by the manufacturer. Briefly, slides were denatured in 70% formamide for 2 min at 65°C, while 10 ml of the Star*FISH probe was denatured for 10 min at 68°C. The probe was preannealed at 37°C for 10 min and then applied to the target area of the slide (22 × 22 mm) on a slide warmer at 37°C. The cover slip was sealed with rubber cement, and the slide was incubated overnight at 37°C in a humid incubator. Slides were then washed in a 50% formamide solution at 45°C and finally processed for immunostaining. First, a layer containing Cy5-avidin and rabbit anti-FITC antibodies was added, and the slide was incubated for 20 min at 37°C. After it was washed in a 2× SSC/0.05% Tween-20 detergent

at 45°C, the slide was hybridized with goat anti-rabbit FITC antibody and incubated again for 20 min at 37°C. After it was washed three times (5 min each) in detergent at 37°C, the slide was counterstained in DAPI II (Vysis, Downers Grove, IL) and stored at –20°C prior to the analysis.

Karyotyping

Hybridized slides were visualized with the PowerGene™ RxFISH system (Applied Imaging, San Jose, CA) connected to a Zeiss Axioplan fluorescence microscope. The slide was scanned with a 40× immersion objective using a triple bandpass filter. Spreads with long, well-separated chromosomes were located, the coordinates on the microscope translator were noted, and the image was visualized with a 100× objective. Four images were saved using the Cy3, Cy5, FITC and DAPI filters in order. Karyotypes were analyzed off-line as described below.

Classification of Chromosome Aberrations

RxFISH has been used in clinical cytogenetics to identify cryptic aberrations that are hard to classify by other methods (16, 17). Unlike 23-color FISH (mFISH) (18), RxFISH technique can be used to visualize intrachanges as well as interchanges. However, RxFISH has too few colors to resolve very complex interchanges involving several different chromosomes such as those observed in cells at the first mitosis after exposure (19). Whereas RxFISH has lower resolution than multicolor banding (mBAND) for the analysis of intrachromosomal exchanges (20, 21), it has the advantage of a full karyotype analysis, while mBAND is restricted to a single chromosome pair. Although some interchanges and intrachanges will remain undetected with the RxFISH technique, the aim was to compare the results for heavy-ion- and γ -ray-exposed samples rather than to provide absolute numbers. We divided aberrations into the categories shown in Table 1, i.e. translocations, dicentric, rings, terminal deletions, interstitial deletions, and pericentric and paracentric inversions. We did not find any acentric fragments in the progeny of the exposed cells. Terminal and interstitial deletions thus refer to shortened chromosomes and were distinguished based on the banding pattern. Further verification of deletions was performed using telomere probes (see below). Complex-type exchanges were classified according to Savage's definition (22) of all configurations resulting from "3 or more breaks in 2 or more chromosomes", and events involving both intra- and interchromosomal exchanges were included in this category.

Telomere Detection

Slides with cells containing chromosome deletions were washed in 2× SSC/0.05% Tween-20 for 15 min at 65°C and rinsed in Tris-buffered saline (TBS). Slides were then hybridized with the telomere PNA FISH probe kit/Cy3 (DakoCytomation, Glostrup, Denmark) following the protocol recommended by the manufacturer. Briefly, slides were fixed in 3.7% formaldehyde, washed in TBS and then incubated 10 min in proteinase K. After rinsing in TBS and dehydrating in a cold ethanol series (70%, 85%, 100%), the PNA probe was added to the target area and the slide was incubated for 5 min at 80°C and then for 30 min at room temperature. Slides were then washed 5 min at 65°C, dehydrated in ethanol, and counterstained with DAPI I (Vysis). The cells were analyzed using the same microscope used for RxFISH, and the Probe module of the PowerGene™ system (Applied Imaging, Houston, TX). The images were acquired with Cy3 and DAPI filters.

Differential Replication Staining

To exclude cells at the first or second mitosis, slides were washed by incubation in 2× SSC/0.05% Tween-20 for 20 min at 37°C and harlequin staining was completed as described previously (23). Briefly, slides were stained in Hoechst 33258 (Sigma) and then exposed to UV light for 20 min. After washing in PBS and dehydration in an ethanol series, cells were counterstained in DAPI and the cells analyzed previously were re-located. Chromosomes at the first mitosis after mitogen stimulation fluo-

resced brightly with uniform intensity, whereas sister chromatids in cells at the second mitosis fluoresced with differential intensity; i.e., they exhibited “harlequin” staining. Cells that had undergone further divisions in the presence of BrdU were easily identified as containing both harlequin chromosomes and chromosomes whose sister chromatids stained uniformly with pale intensity. In general, it was not possible to distinguish third-cycle cells from fourth-cycle cells reliably using this method, and no such attempt was made.

RESULTS

Chromosomal Aberrations Visualized by RxFISH

We found that over 90% of the cells had reached at least the third mitosis 144 h after *in vitro* growth stimulation, and any remaining first- and second-division cells were excluded from the analysis using differential replication staining. Anderson *et al.* (24) cultivated human lymphocytes for a much longer period, and they observed no significant differences in the yield of stable radiation-induced chromosome aberrations from days 7 to 41 in culture. Figure 1A shows an RxFISH-painted cell from the population originally exposed to 3 Gy of iron ions. The karyotype of this cell, which includes a reciprocal translocation, is displayed in Fig. 1B. Examples of intrachromosomal exchanges visualized by RxFISH in the progeny of cells exposed to iron ions are shown in Fig. 1c.

Dose–Response Curves for the Induction of Different Aberrations

Although HZE particles are much more effective than γ rays in the induction of chromosomal aberrations in human lymphocytes (5), we found similar fractions of stable, transmissible-type aberrations after three or more replication rounds (Fig. 2B). However, a higher fraction of unstable aberrations was observed in the cells originating from the population exposed to heavy ions (Fig. 2A). We observed aberrant karyotypes in 1% of the unirradiated cells, whereas around 60% of karyotypes were aberrant in the progeny of cells exposed to 3 Gy of iron ions. Although the analysis was restricted to cells reaching the third cell division or later after exposure, we still observed a fraction of unstable, asymmetrical aberrations that accounted for about 10% and 40% of the aberrant cells from the populations exposed to γ rays or iron ions, respectively. Dose–response curves for the induction of each chromosome aberration type are shown in Fig. 3. Unstable aberrations included dicentrics that were involved in either simple asymmetrical interchanges or complex-type exchanges, along with centric rings, and terminal deletions (Fig. 3D). The majority of the interchanges were reciprocal translocations (Fig. 3A). Ostensibly stable intrachanges included interstitial deletions as well as pericentric and paracentric inversions (Fig. 3B). Complex-type exchanges (Fig. 3C) included insertions, non-reciprocal exchanges, and multi-break rearrangements involving both inter- and intrachanges. Complex exchanges accounted for only 27% and 17% of the interchromosomal

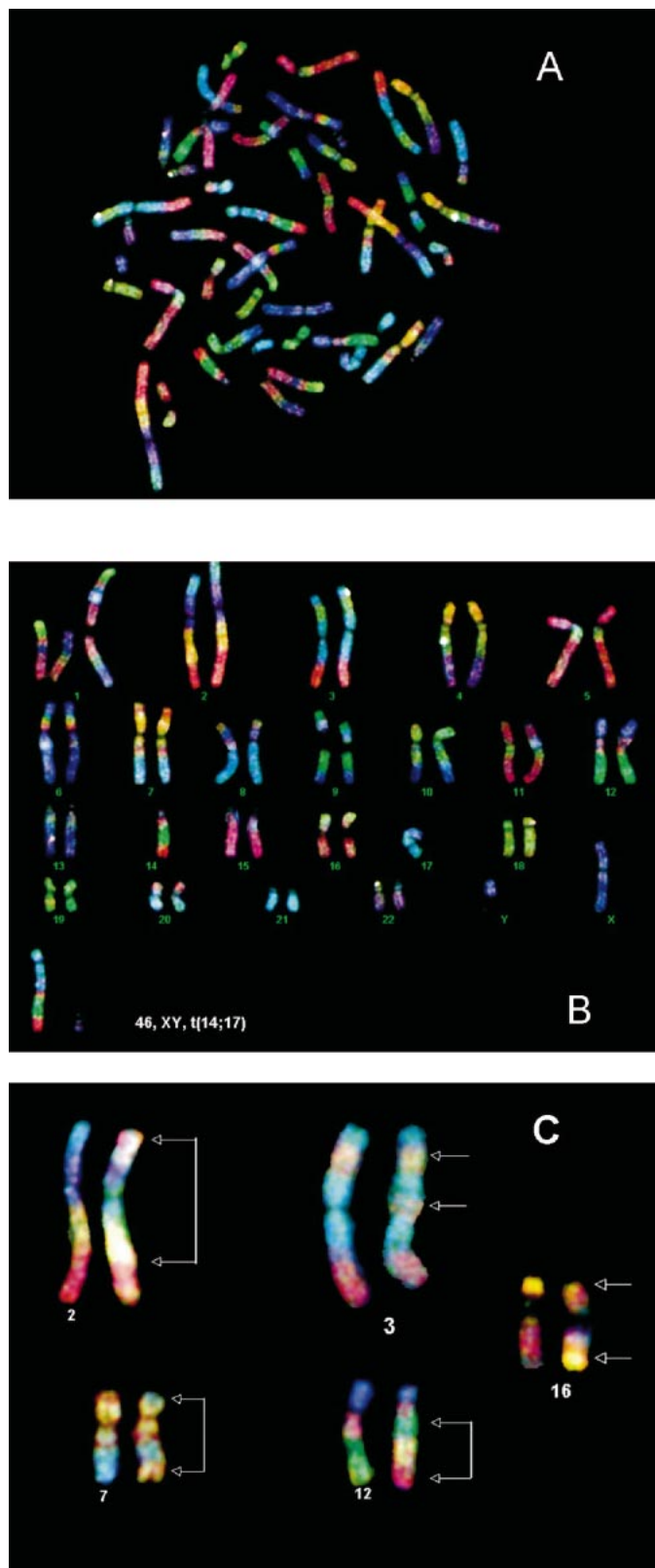


FIG. 1. Aberrations in human lymphocytes, visualized by RxFISH. Panel A: A metaphase cell from the progeny of the population exposed to 3 Gy of iron ions. Panel B: Karyotype of cell shown in panel A, showing a reciprocal translocation involving chromosomes 14 and 17. Panel C: Examples of inter- and intra-arm intrachromosomal exchanges in the progeny of the lymphocytes exposed to iron ions or γ rays. The panel includes pericentric inversions in chromosomes 2, 7 and 16 and paracentric inversions in chromosomes 3 and 14.

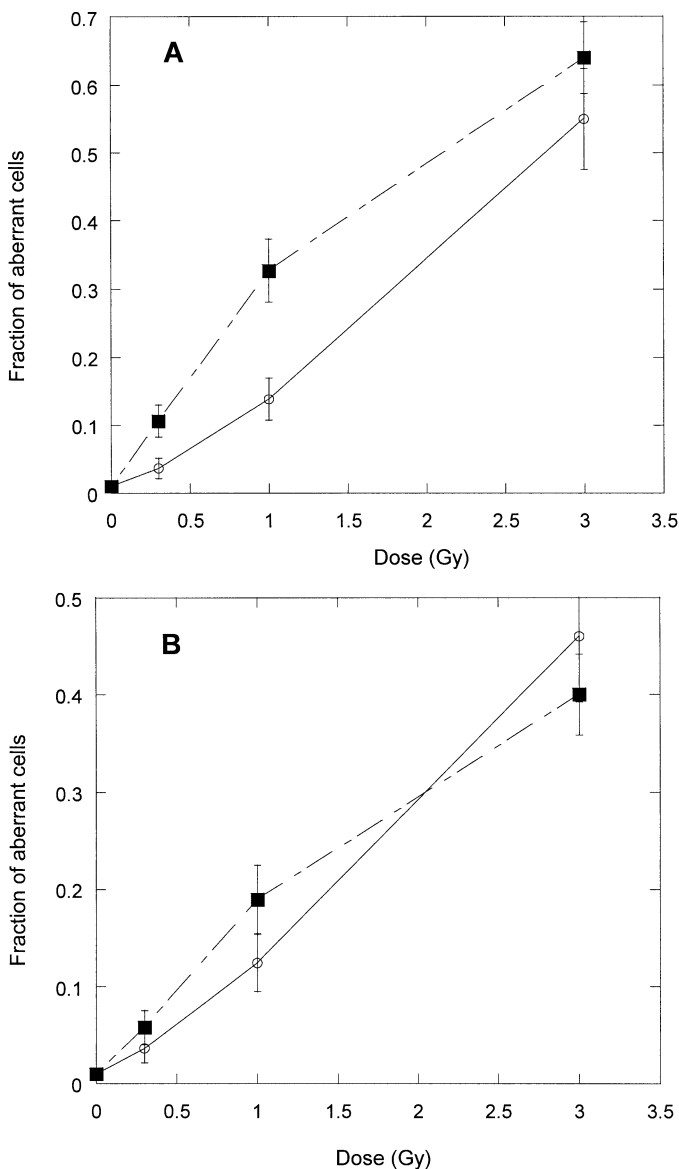


FIG. 2. Induction of aberrant karyotypes in the progeny of human lymphocytes exposed to γ rays (○) or iron ions (■). Metaphase cells were harvested 144 h after exposure, and aberrations were analyzed by RxFISH. Bars represent standard errors of the mean values. Lines are guides for the eye. Panel A: Fraction of aberrant karyotypes, including cells carrying unstable rearrangements; panel B: fraction of cells carrying only stable, transmissible aberrations.

exchanges induced by 3 Gy of iron ions and γ rays, respectively. This compares with approximately 70% and 24% complex exchanges measured at the first cell cycle after exposure to 3 Gy of iron ions and γ rays, respectively, when human lymphocytes were assessed using multi-fluor FISH (25). This suggests that most of the complex-type exchanges induced by HZE particles are unstable and lead to cell death within the first three replicative cell cycles. It is also possible that some of the aberrations observed using PCC in human lymphocytes (5, 25) would not be visible at the first mitosis after exposure. The relative biological effectiveness (RBE) of iron ions for the induction of inter-

changes in the progeny of exposed cells is much less than that measured in cells directly after exposure, where an RBE > 4 has been determined after a low dose using FISH painting probes for two or three chromosomes (5, 25). Iron ions were only slightly more effective than γ rays in the induction of stable intrachanges in progeny cells (Fig. 2B), confirming previous observations using multicolor banding (mBAND) in lymphocytes exposed to iron ions and analyzed at the first cell cycle after exposure (26). The RBE is higher for complex exchanges, although, as noted above, many complex exchanges induced by iron ions are lost after three or more cell cycles.

Terminal Deletions

Interestingly, the highest RBE was for truncated chromosomes, apparently terminal deletions (Fig. 2D). Terminal deletions accounted for about 10% of all aberrations observed in the progeny of cells exposed to iron ions, whereas only two events were positively identified as terminal deletions in the 84 aberrant cells from the population exposed to γ rays (Table 1). To confirm that these chromosomes were indeed missing a telomere, we rehybridized the slides using telomere PNA probes, and this resulted in a positive identification of telomere loss as well as identification of interstitial deletions (Fig. 4).

DISCUSSION

Using RxFISH combined with telomere probes, we have demonstrated that HZE particles induce true terminal deletions of a chromosome and that chromosomes missing a telomere can be transmitted through multiple cell divisions. Although it has been shown that radiation can induce terminal deletions, especially in repair-deficient cells (27), this is the first evidence that these types of aberrations can be transmitted. It is likely that the cells containing telomere-deficient chromosomes will either senesce or undergo B/F/B cycles, promoting genetic instability. Bridging of telomere-deficient chromosomes is a major mutational mechanism in cancer cells (28).

Late morbidity associated with exposure to HZE particles is one of the major health concerns for manned interplanetary space missions (29). The frequency of chromosomal aberrations in the progeny of cells exposed to radiation may represent a useful surrogate end point of latent health risks to astronauts (30). However, additional information is needed on specific types of aberrations that have been correlated with mechanisms of carcinogenesis. Our results show that the RBE for heavy ions is lower for the daughters of irradiated normal human cells than in the population originally exposed to radiation. This is caused by the loss of cells carrying complex-type exchanges, which predominates after exposure to high-LET heavy ions. For the progeny of cells exposed to iron ions, terminal deletions are the only aberration type that presents the very high RBE that is con-

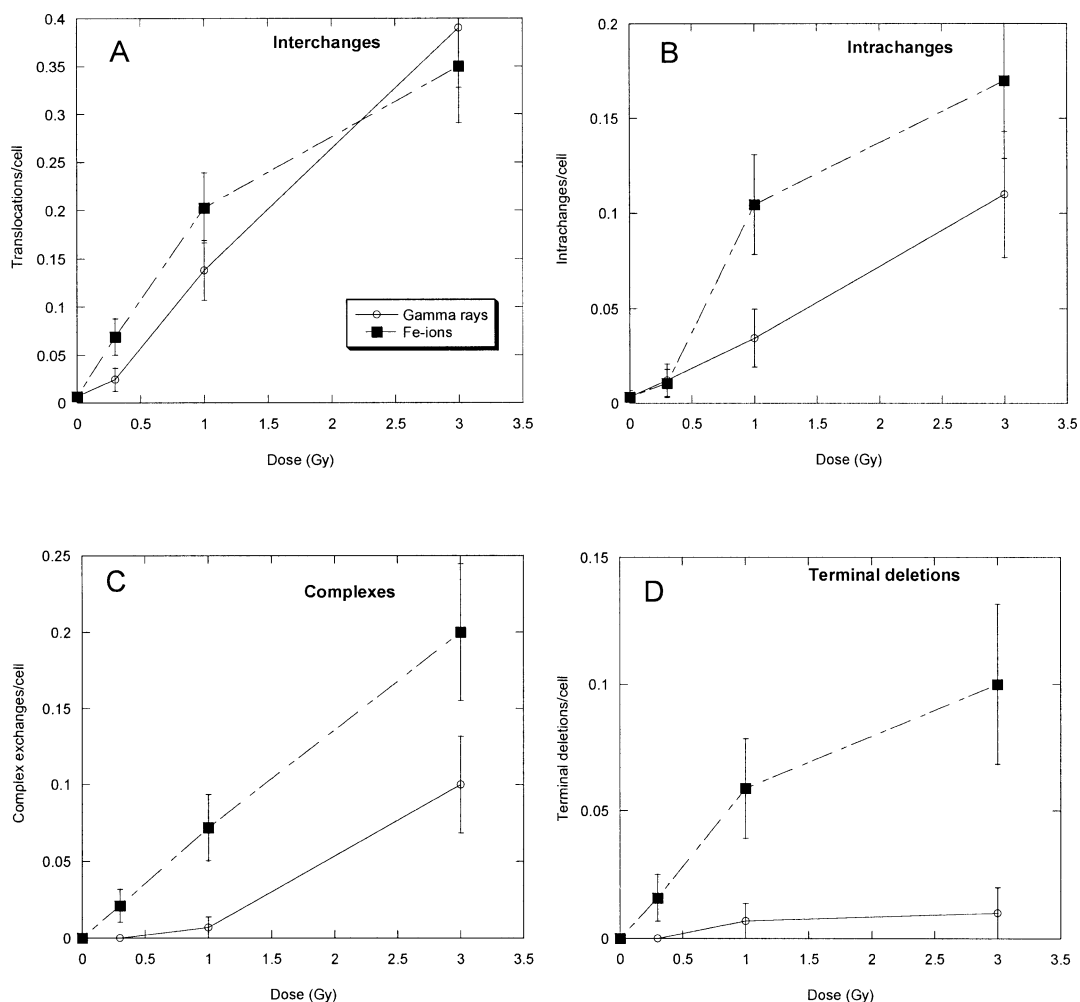


FIG. 3. Dose–response curves for the induction of chromosomal aberrations in the progeny of cells exposed to γ rays (○) or iron ions (■). Metaphase cells were harvested 144 h after exposure, and aberrations were analyzed by RxFISH. Bars represent standard errors of the mean values. Lines are guides for the eye. Panel A: Stable interchanges (translocations); panel B: stable intrachanges (interstitial deletions or inversions); panel C: complex-type exchanges; panel D: terminal deletions.

TABLE 1
Chromosomal Aberrations Scored in Human Lymphocytes Harvested 144 h after Exposure to Radiation

Radiation	Dose (Gy)	Cells scored	Aberrant cells		Trans-locations	Dicentric ^c	Terminal deletions	Interstitial deletions	Inversions ^d	Rings	Complex exchanges ^e	Total aberrations
			(stable) ^a	(unstable) ^b								
Gamma rays	0.0	297	3	0	2	0	0	1	0	0	0	3
	0.3	164	6	0	4	0	0	1	1	0	0	6
	1.0	145	18	2	20	2	1	3	2	0	1	29
	3.0	100	46	9	39	9	1	5	6	1	10	71
Iron ions	0.3	189	11	9	13	6	3	1	1	0	4	28
	1.0	153	29	21	31	11	9	9	7	1	11	79
	3.0	100	40	24	35	20	10	8	9	2	20	104

^a Karyotypes containing transmissible aberrations only.

^b Karyotypes containing non-transmissible aberrations.

^c Including complex-type dicentric.

^d Including interarm and intra-arm.

^e Including inter- plus intrachromosomal complex rearrangement.

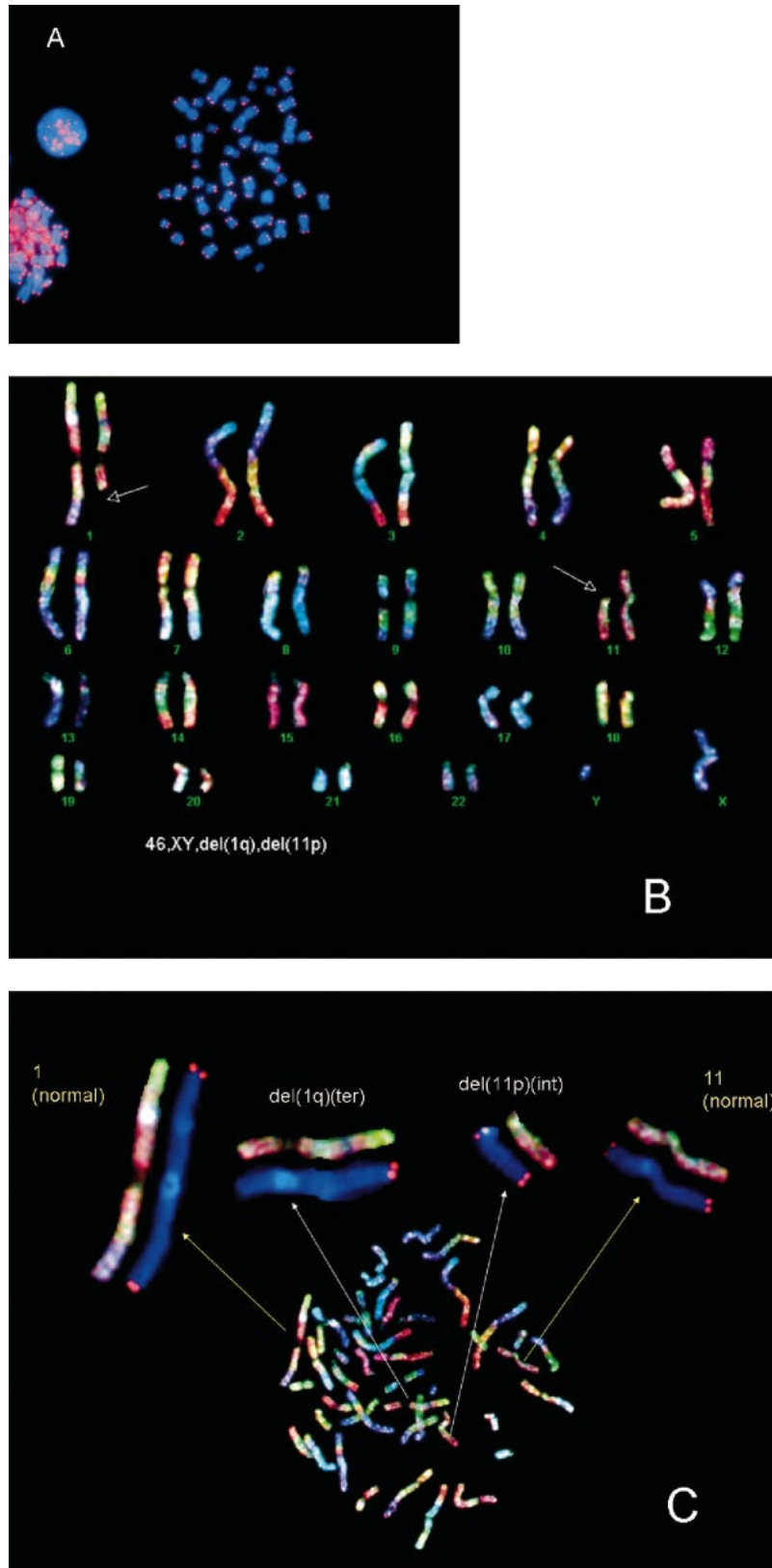


FIG. 4. Identification of terminal deletions using telomeric PNA probes. Panel A: A typical metaphase painted with the PNA probe. Panel B: A daughter cell from the population exposed to iron ions containing two deletions in chromosomes 1 and 11. The lack of banding on 11p makes it impossible to positively classify the deletion as terminal or interstitial, whereas the deletion in 1q appears to be terminal because the last color band in 1q is missing. Panel C: Telomere painting using PNA probes allows positive identification of the deletion in chromosome 1 as terminal and the deletion in chromosome 11 as interstitial.

sistent with the expected values for late end points such as cancer (31, 32). Interestingly, heavy-ion-induced chromosomal instability in human fibroblasts appears to be associated with rearrangements involving telomere regions (33, 34). No significant shortening of telomeres was detected in those cells (35), but it has recently been shown that the loss of a single telomere in cancer cells can result in instability in multiple chromosomes (36). In addition, telomere shortening is associated with aging in normal human cells (37, 38). HZE particles are particularly effective in inducing end points related to accelerated aging such as cataractogenesis (39) and central nervous system damage (40). In fact, heavy ions are so effective in inducing accelerated-aging effects that an RBE is hard to define, given the lack of effects after low doses of sparsely ionizing radiation (29). We therefore contend that terminal deletions and transmission of telomere-free chromosomes may be key events in determining late effects after exposure to HZE particles.

ACKNOWLEDGMENTS

We thank the crew of the NASA Space Radiation Laboratory at Brookhaven National Laboratory for their support during irradiations and Ms. V. Willingham for technical assistance. This work was supported by the NASA Space Radiation Health Program and the Office of Science (BER), U.S. Department of Energy, Interagency Agreement No. OE-AI03-05ER64088 (FC). MD was supported by the University Space Research Association.

Received: May 5, 2005; accepted: August 17, 2005

REFERENCES

1. M. N. Cornforth and J. S. Bedford, Ionizing radiation damage and its early development in chromosomes. *Adv. Radiat. Biol.* **17**, 423–497 (1993).
2. G. Obe, P. Pfeiffer, J. R. K. Savage, C. Johannes, W. Goedecke, P. Jeppesen, A. T. Natarajan, W. Martinez-Lopez, G. A. Folle and M. E. Drets, Chromosomal aberrations: Formation, identification and distribution. *Mutat. Res.* **504**, 17–36 (2002).
3. H. Wu, K. George and T. C. Yang, Estimate of true incomplete exchanges using fluorescence *in situ* hybridization with telomere probes. *Int. J. Radiat. Biol.* **73**, 521–527 (1998).
4. J. Fomina, F. Darroudi, J. J. Boeri and A. T. Natarajan, Discrimination between complete and incomplete chromosome exchanges in X-irradiated human lymphocytes using FISH with pan-centromeric and chromosome specific DNA probes in combination with telomeric PNA probe. *Int. J. Radiat. Biol.* **76**, 807–813 (2000).
5. K. George, M. Durante, V. Willingham, H. Wu, T. C. Yang and F. A. Cucinotta, Biological effectiveness of accelerated particles for the induction of chromosome damage measured in metaphase and interphase human lymphocytes. *Radiat. Res.* **160**, 425–435 (2003).
6. M. Durante, Y. Furusawa, K. George, G. Gialanella, O. Greco, G. Grossi, N. Matsufuji, M. Pugliese and T. C. Yang, Rejoining and misrejoining of radiation-induced chromatin breaks. IV. Charged particles. *Radiat. Res.* **149**, 446–454 (1998).
7. H. Wu, M. Durante, Y. Furusawa, K. George, T. Kawata and F. A. Cucinotta, Truly incomplete and complex exchanges in prematurely condensed chromosomes of human fibroblasts exposed *in vitro* to energetic heavy ions. *Radiat. Res.* **160**, 418–424 (2003).
8. R. S. Maser and R. A. DePinho, Connecting chromosomes, crisis, and cancer. *Science* **297**, 565–569 (2002).
9. D. M. Feldser, J. A. Hackett and C. W. Greider, Telomere dysfunction and the initiation of genome instability. *Nat. Rev. Cancer* **3**, 623–627 (2003).
10. S. E. Artandi, S. Chang, S. L. Lee, S. Alson, G. J. Gottlieb, L. Chin and R. A. DePinho, Telomere dysfunction promotes non-reciprocal translocations and epithelial cancers in mice. *Nature* **406**, 641–645 (2000).
11. D. Gisselsson, T. Jonsson, A. Petersén, B. Strömbeck, P. Dal Cin, M. Höglund, F. Mitelman, F. Mertens and N. Mandahl, Telomere dysfunction triggers extensive DNA fragmentation and evolution of complex chromosome abnormalities in human malignant tumors. *Proc. Natl. Acad. Sci. USA* **98**, 12683–12688 (2001).
12. R. M. Anderson, D. L. Stevens and D. T. Goodhead, M-FISH analysis shows that complex chromosome aberrations induced by alpha-particle tracks are cumulative products of localized rearrangements. *Proc. Natl. Acad. Sci. USA* **99**, 12167–12172 (2002).
13. M. P. Hande, T. V. Azizova, C. R. Geard, L. E. Burak, C. R. Mitchell, V. F. Khokhryakov, E. K. Vasilenko and D. J. Brenner, Past exposure to densely ionizing radiation leaves a unique permanent signature in the genome. *Am. J. Hum. Genet.* **72**, 1162–1170 (2003).
14. S. Müller, P. C. O'Brien, M. A. Ferguson-Smith and J. Wienberg, Cross-species colour segmenting: A novel tool in human karyotype analysis. *Cytometry* **33**, 445–452 (1998).
15. C. Zeitlin, L. Heilbronn and J. Miller, Detailed characterization of the 1087 MeV/nucleon iron-56 beam used for radiobiology at the alternating gradient synchrotron. *Radiat. Res.* **149**, 560–569 (1998).
16. M. R. Teixeira, Combined classical and molecular cytogenetic analysis of cancer. *Eur. J. Cancer* **38**, 1580–1584 (2002).
17. T. Liehr, H. Starke, A. Weise, H. Lehrer and U. Claussen, Multicolor FISH probe sets and their applications. *Histol. Histopathol.* **19**, 229–237 (2004).
18. E. Schröck, S. du Manoir, T. Veldman, B. Schoell, J. Wienberg, M. A. Ferguson-Smith, Y. Ning, D. H. Ledbetter, I. Bar-Am and T. Ried, Multicolor spectral karyotyping of human chromosomes. *Science* **273**, 494–497 (1996).
19. M. N. Cornforth, Analyzing radiation-induced complex chromosome rearrangements by combinatorial painting. *Radiat. Res.* **155**, 643–659 (2001).
20. I. Chudoba, G. Hickmann, T. Friedrich, A. Jauch, P. Kozlowski and G. Senger, mBAND: a high resolution multicolor banding technique for the detection of complex intrachromosomal aberrations. *Cytogenet. Genome Res.* **104**, 390–393 (2004).
21. M. Horstmann and G. Obe, CABAND: Classification of aberrations in multicolor banded chromosomes. *Cytogenet. Genome Res.* **103**, 24–27 (2003).
22. J. R. K. Savage, Reflections and meditations upon complex chromosomal exchanges. *Mutat. Res.* **512**, 93–109 (2002).
23. K. George, H. Wu, V. Willingham, Y. Furusawa, T. Kawata and F. A. Cucinotta, High- and low-LET induced chromosome damage in human lymphocytes: A time-course of aberrations in metaphase and interphase. *Int. J. Radiat. Biol.* **77**, 175–183 (2001).
24. R. M. Anderson, S. J. Marsden, S. J. Paice, A. E. Bristow, M. A. Kadhim, C. S. Griffin and D. T. Goodhead, Transmissible and non-transmissible complex chromosome aberrations characterized by three-color and mFISH define a biomarker of exposure to high-LET alpha particles. *Radiat. Res.* **159**, 40–48 (2003).
25. M. Durante, K. George, H. Wu and F. A. Cucinotta, Karyotypes of human lymphocytes exposed to high-energy iron ions. *Radiat. Res.* **158**, 581–590 (2002).
26. C. Johannes, M. Horstmann, M. Durante, I. Chudoba and G. Obe, Chromosome intrachanges and interchanges detected by multicolor banding in lymphocytes: Searching for clastogen signatures in the human genome. *Radiat. Res.* **161**, 540–548 (2004).
27. M. N. Cornforth and J. S. Bedford, On the nature of a defect in cells from individuals with ataxia-telangiectasia. *Science* **227**, 1589–1591 (1985).
28. Y. Stewenius, L. Gorunova, T. Jonson, N. Larsson, M. Hoglund, N. Mandahl, F. Mertens, F. Mitelman and D. Gisselsson, Structural and numerical chromosome changes in colon cancer develop through

- telomere-mediated anaphase bridges, not through mitotic multipolarity. *Proc. Natl. Acad. Sci. USA* **102**, 5441–5446 (2005).
29. NCRP, *Radiation Protection Guidance for Activities in Low-Earth Orbit*. Report No. 132, National Council on Radiation Protection and Measurements, Bethesda, MD, 2000.
 30. M. Durante, S. Bonassi, K. George and F. A. Cucinotta, Risk estimation based on chromosomal aberrations induced by radiation. *Radiat. Res.* **156**, 662–667 (2001).
 31. E. L. Alpen, P. Powers-Risius, S. B. Curtis and R. DeGuzman, Tumorigenic potential of high-Z, high-LET charged-particle radiations. *Radiat. Res.* **136**, 382–391 (1993).
 32. E. A. Blakely and A. Kronenberg, Heavy-ion radiobiology: New approaches to delineate mechanisms underlying enhanced biological effectiveness. *Radiat. Res.* **150** (Suppl.), S126–S145 (1998).
 33. L. Sabatier, B. Dutrillaux and M. B. Martin, Chromosomal instability. *Nature* **357**, 548 (1992).
 34. M. B. Martin, L. Sabatier, M. Ricoul, A. Pinton and B. Dutrillaux, Specific chromosome instability induced by heavy ions: A step towards transformation of human fibroblasts? *Mutat. Res.* **285**, 229–237 (1993).
 35. L. Sabatier, J. Lebeau and B. Dutrillaux, Chromosomal instability and alterations of telomeric repeats in irradiated human fibroblasts. *Int. J. Radiat. Biol.* **66**, 611–613 (1994).
 36. L. Sabatier, M. Ricoul, G. Pottier and J. P. Murnane, The loss of a single telomere can result in instability of multiple chromosomes in a human tumor cell line. *Mol. Cancer Res.* **3**, 139–150 (2005).
 37. J. W. Shay and W. E. Wright, Aging. When do telomeres matter? *Science* **291**, 839–840 (2001).
 38. J. Campisi, Senescent cells, tumor suppression, and organismal aging: good citizens, bad neighbors. *Cell* **120**, 513–522 (2005).
 39. F. A. Cucinotta, F. K. Manuel, J. Jones, G. Iszard, J. Murrey, B. Djojonegro and M. Wear, Space radiation and cataracts in astronauts. *Radiat. Res.* **156**, 460–466 (2001).
 40. N. A. Denisova, B. Shukitt-Hale, B. M. Rabin and J. A. Joseph, Brain signaling and behavioral responses induced by exposure to ⁵⁶Fe-particle radiation. *Radiat. Res.* **158**, 725–734 (2002).